

8-27-2013

Mesospheric Density Climatologies Determined at Midlatitudes Using Rayleigh Lidar

David L. Barton
Utah State University

Vincent B. Wickwar
Utah State University

Leda Sox
Utah State University

Joshua P. Herron
Utah State University

Follow this and additional works at: https://digitalcommons.usu.edu/atmlidar_post



Part of the [Physics Commons](#)

Recommended Citation

Barton, David L.; Wickwar, Vincent B.; Sox, Leda; and Herron, Joshua P., "Mesospheric Density Climatologies Determined at Midlatitudes Using Rayleigh Lidar" (2013). International Association of Geomagnetism and Aeronomy; Mexico; 2013. *Posters*. Paper 21.

https://digitalcommons.usu.edu/atmlidar_post/21

This Poster is brought to you for free and open access by the Green Beam (Rayleigh-Scatter LIDAR) at DigitalCommons@USU. It has been accepted for inclusion in Posters by an authorized administrator of DigitalCommons@USU. For more information, please contact digitalcommons@usu.edu.



Abstract

The original Rayleigh-scatter lidar that operated at the Atmospheric Lidar Observatory (ALO; 41.7°N, 111.8°W) in the Center for Atmospheric and Space Sciences (CASS) on the campus of Utah State University (USU), collected 11 years of data between 1993 and 2004. From Rayleigh lidar photon-count returns, relative densities throughout the mesosphere, from 45 to 90 km, were determined. Using these relative densities, three climatologies are derived, each using a different density normalization method at 45 km: the first method normalized the relative densities to a constant; the second normalized them to the NRLMSISE00 empirical model; and the third normalized them to the CPC analyses, a first principles, assimilative, meteorological model. From there, the average density profile for each night of the composite year is found by averaging the nighttime density profiles in a multi-year, 31-day window centered on that particular night. From these three density climatologies, some different and many common features in the mesospheric densities are evident. In the future, with improvements to the lidar, it will be possible to provide an absolute normalization for the density profiles.

Introduction

Rayleigh lidar has been the major ground-based technique for making mesospheric observations of absolute temperatures. Figure 1 shows the green (532 nm) laser beam coming out of the Atmospheric Lidar Observatory on the campus USU. Figure 2 shows the 11-year temperature climatology and Figure 3 follows up with monthly averages (Herron, 2007). These show very distinct variations in both time and altitude.

The Rayleigh lidar observations also provide relative neutral number densities. These densities have been much less studied because they are relative, not absolute. Here, we explore the neutral densities using 3 different normalizations at 45 km. The first, labeled “USU”, is a constant value throughout the year. The second, labeled “MSIS”, uses densities from the MSISE00 model (Picone et al., 2002) for each day of the year. This normalization is used because so many people use the MSISE90 model. The third, labeled “CPC”, is an older meteorological model from the Climate Prediction Center (Gelman, 1986). Its values were applied to each night of data. Additional normalizations will be applied in the future. The significant point is that despite the different normalizations, many of the same features are observed in all three cases.

Rayleigh Lidar at ALO



Photo by Joseph Slansky

Figure 1. Photo of the running Rayleigh lidar system at ALO.

Temperature Climatology

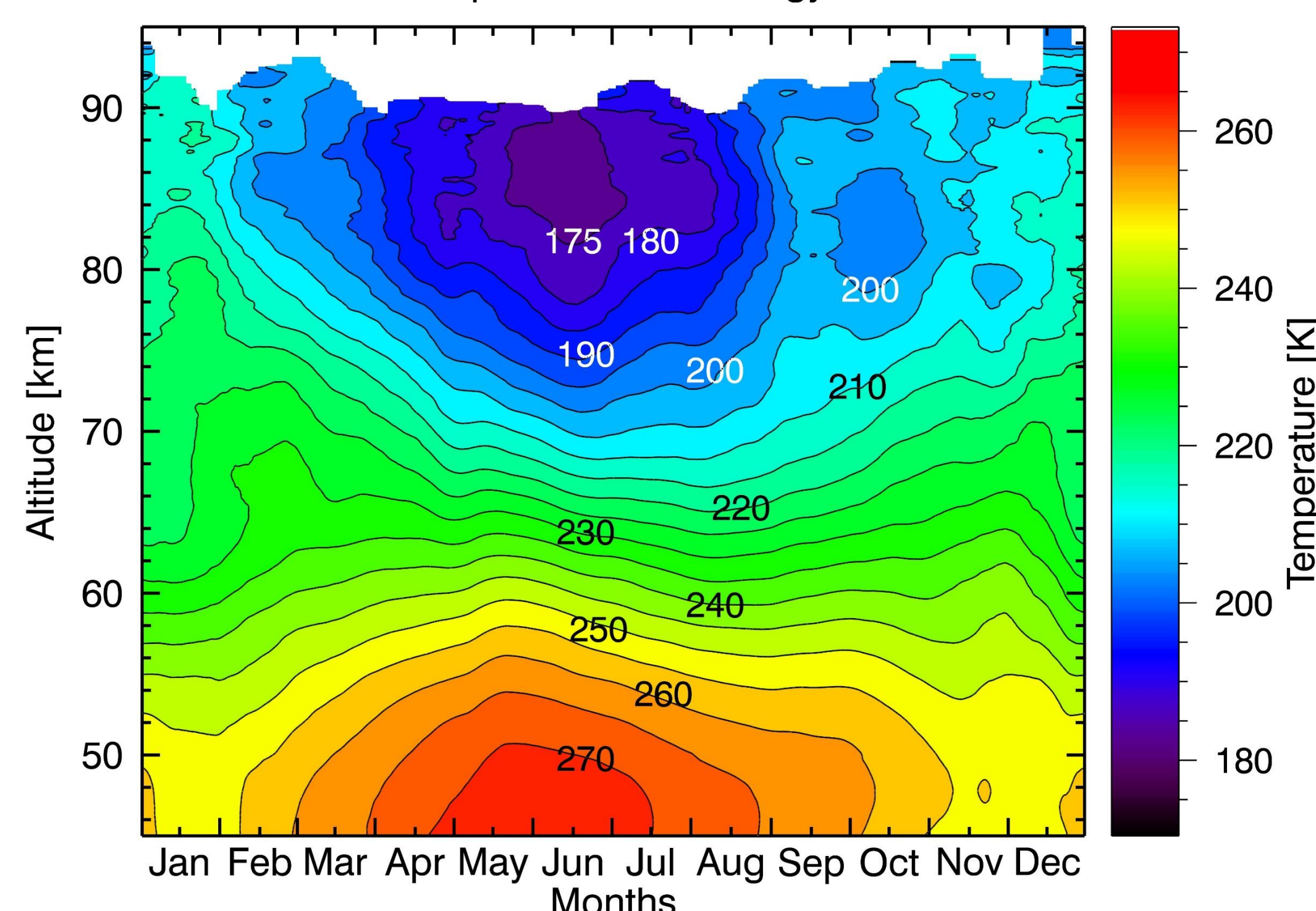


Figure 2. 11- year ALO temperature climatology

Monthly Temperature Averages

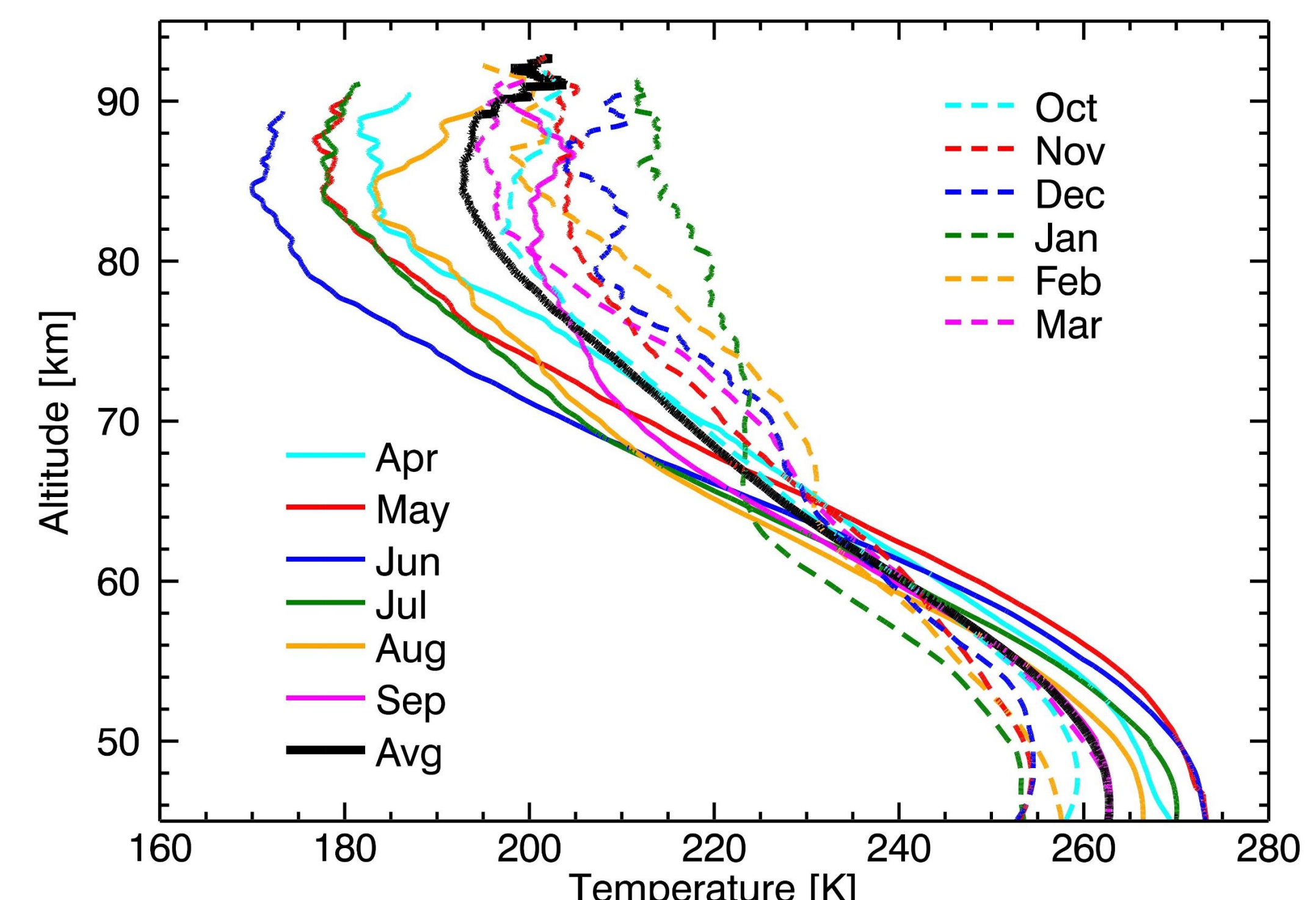


Figure 3. 11-year monthly temperature averages

Analysis Procedures

Data Reduction

To calculate the relative densities from the lidar photon counts, the 2 minute raw data profiles were averaged for the entire night then the background was subtracted to get a nightly signal profile. The background subtracted signal was then multiplied by the range squared to get densities.

Normalization

Three methods were used to normalize the density profiles at 45 km (Figure 4-6). The “USU” method normalized the densities to $4 \times 10^{22} \text{ m}^{-3}$. The “MSIS” method used values from the NRL MSISE00 model to normalize each day of the composite year. The “CPC” method used CPC analysis data to normalize each of the 964 number density profiles. All night averages were averaged over 31 days by 11 years, creating a composite year average.

Density at 45 km

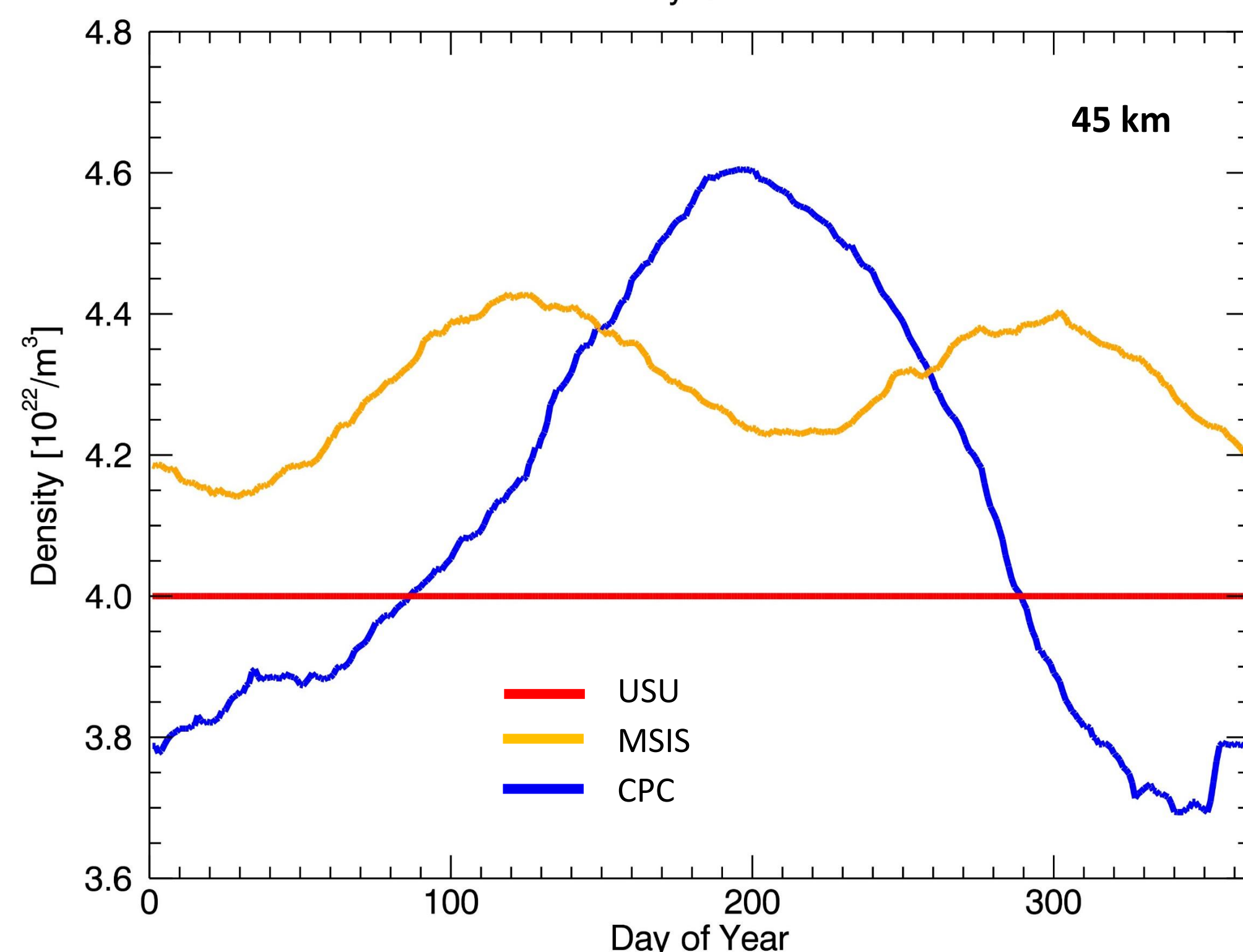


Figure 4. At 45 km, we see a straight line for the USU Density due to the number density being normalized $4 \times 10^{22} \text{ m}^{-3}$. A semiannual oscillation is apparent in the MSIS normalization with peaks apparent around days 120 (April/May) and 300 (October/November). The CPC number density shows that there is an annual oscillation with the peak located around day 180.

Density at 65 km

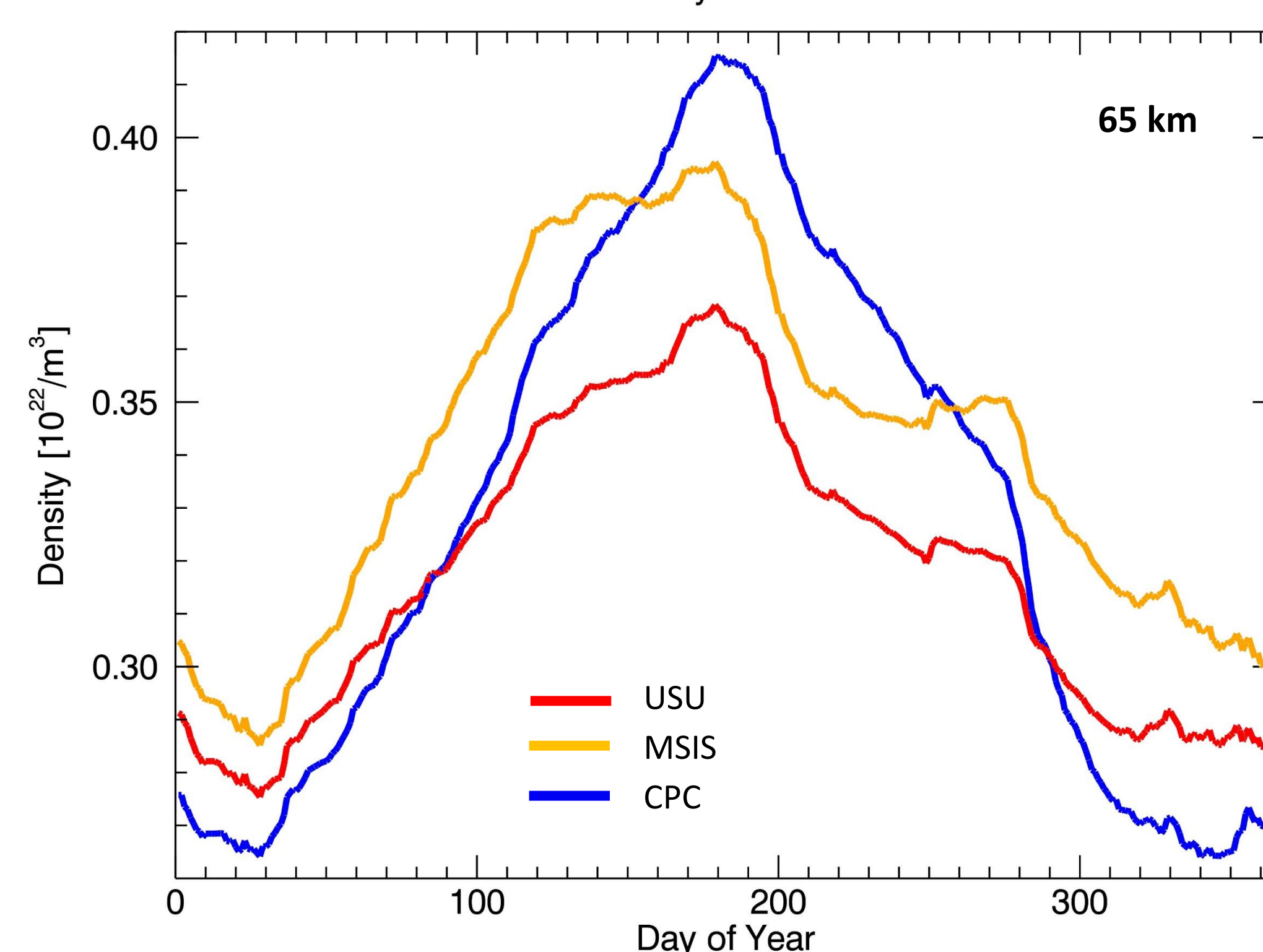


Figure 5. At 65 km, annual variation is apparent in all models. Semiannual variation is still apparent and the semi annual oscillation for MSIS is not as pronounced as it was at 65 km but still evident. The second peak has shifted to around day 270 (September/October). Semiannual variation in the USU density follows a pattern similar to the MSIS normalization. CPC maintains the shape that was apparent at 45 km or so than the other models.

Density at 85 km

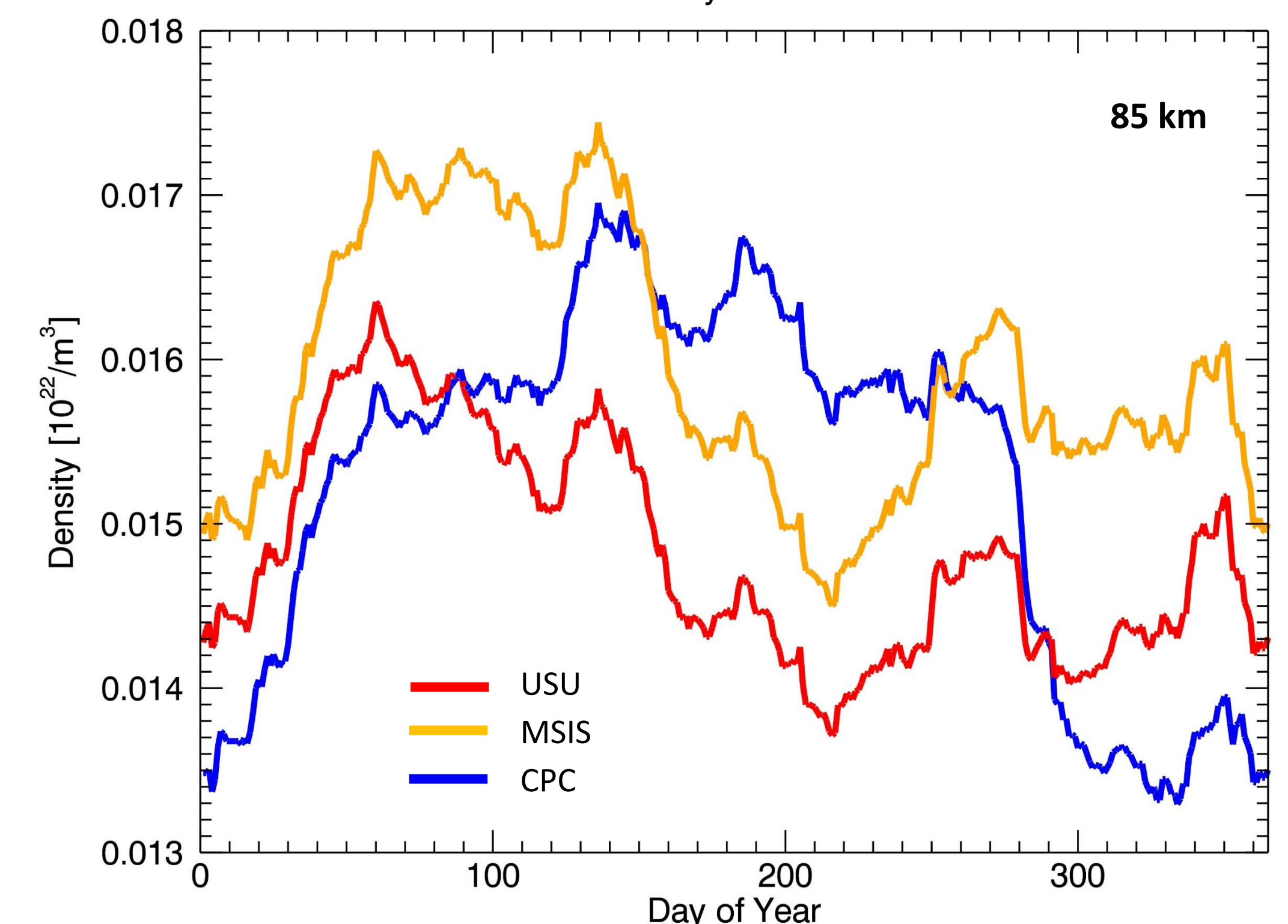


Figure 6. At 85 km, the peaks for each model have shifted to an earlier time in the season and the fall equinox peaks are more pronounced. Also a peak at the winter solstice has become apparent. CPC is still varying on an annual level where as MSIS and USU vary on a semi annual level. All models vary seasonally and become rather noisy at higher altitudes.

Percent Variation of the Number Density

The percent variation of the number density from the composite year mean was found by taking $(d_i - D)/D$, where d_i is the nightly averaged density profile and D is the corresponding day of the year profile from the composite year average. This percent variation was then plotted over the 31 day by 11 year composite average. Note the structures that are present in all plots in Figures 7-9. The seasonal variations show an intense positive (red/yellow) percent difference structure located in the summer months. There is also a slightly negative (dark blue) density variation column that exists in the winter and late fall months. Within this column there is a structure of even more negative (purple) density variations that is apparent in all of the models. There is a slightly negative (dark blue) density region located around the summer months and into early September that propagates downward from 90 km to around 70 km. This structure is easily found in the MSIS and USU plots (Figure 7 and 8) but is not as strong in the CPC version (Figure 9). During the spring and summer months (beginning in March and going to the end of July), the percent variation of density is slightly positive (green) throughout all altitudes. Figures 10-12 show curves of monthly averages from the composite year of percent variation for each of the normalization methods

Mesospheric Densities (Continued)

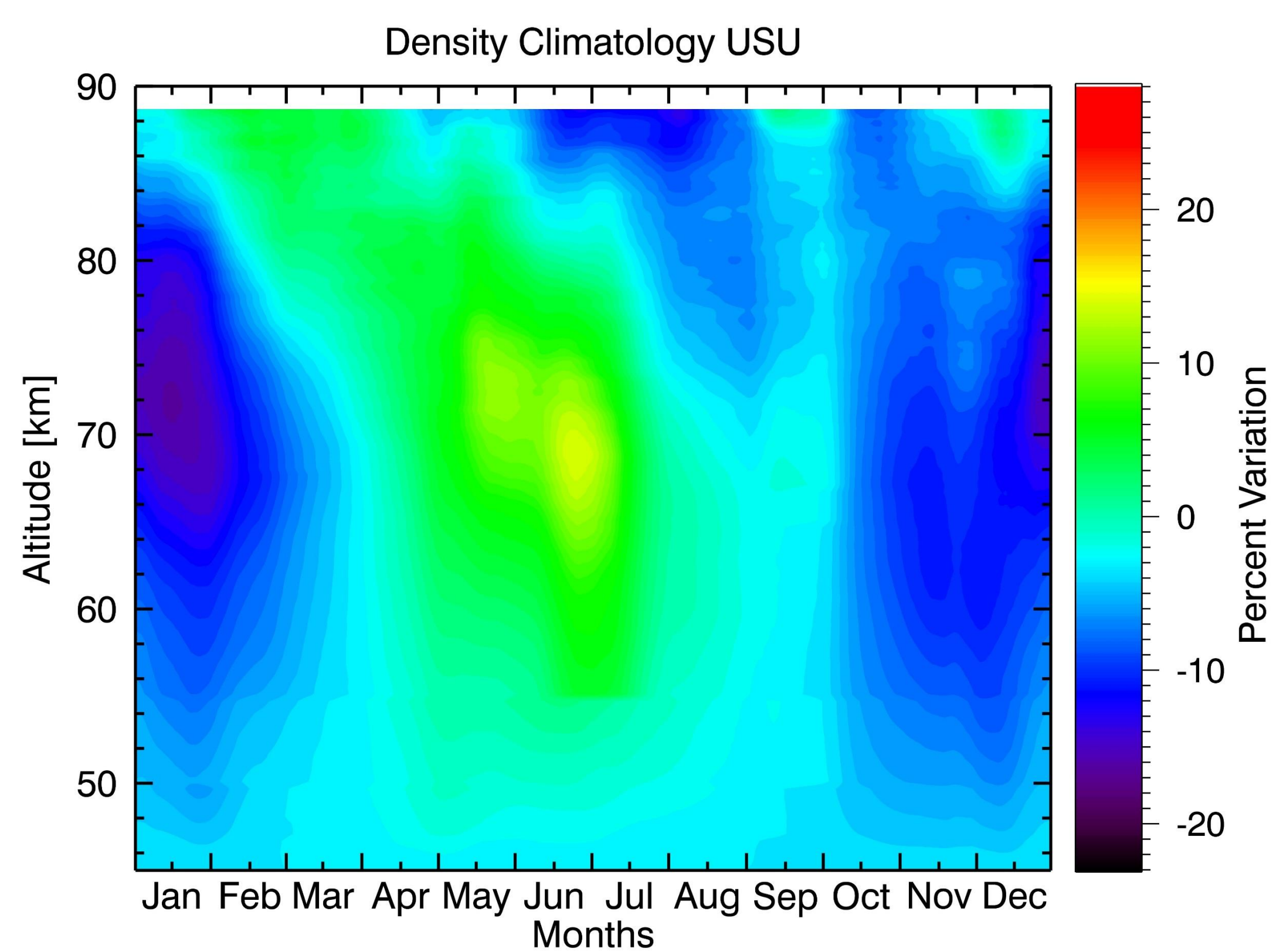


Figure 7. USU Method. The lowest density variation is located around December and January. Notice the rapid change in density from winter to summer. There is also a low density variation located around the summer months at high altitude that extends down to about 75 km. The highest variation of density is located over June around the summer solstice at 70 km.

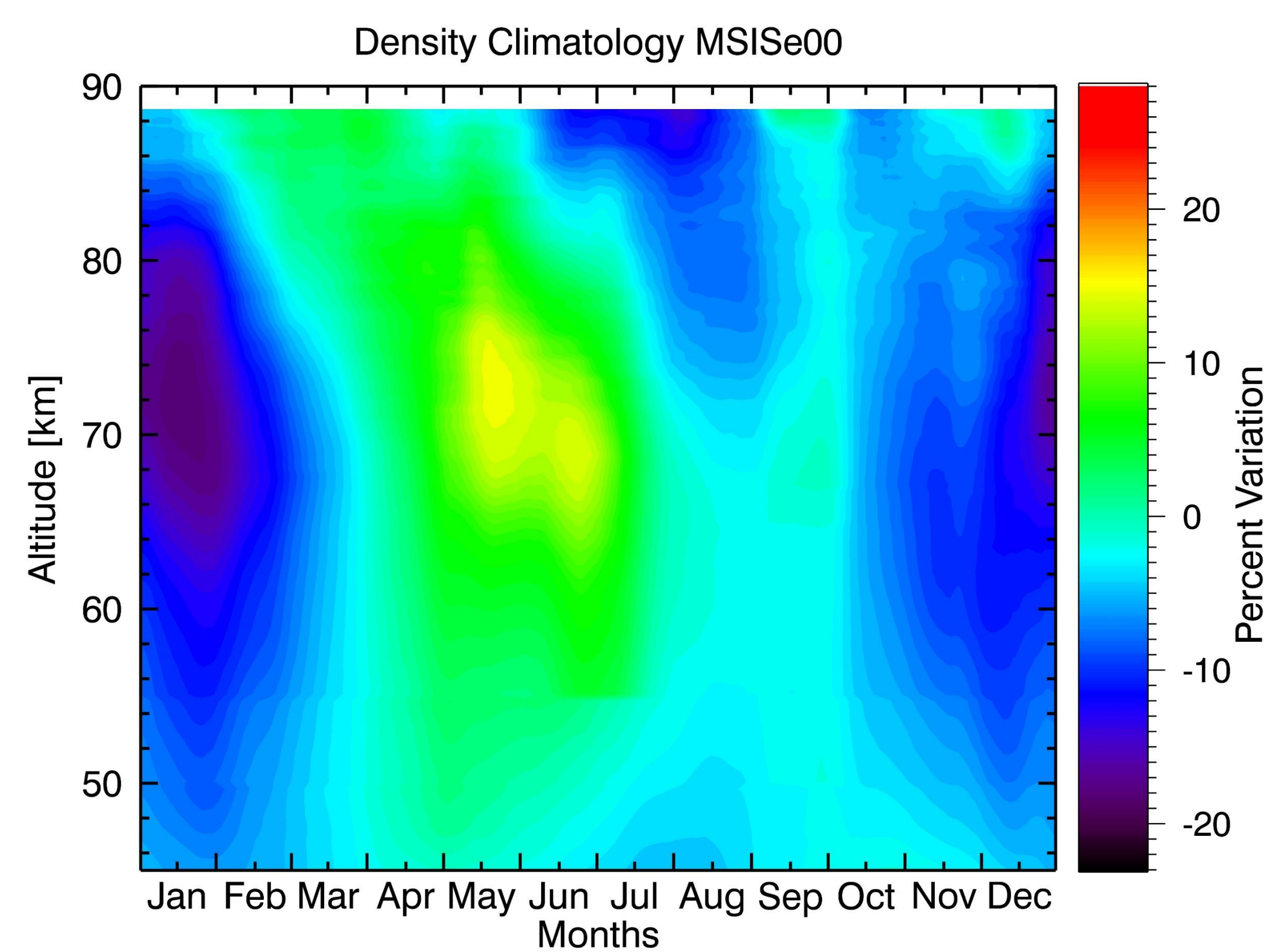


Figure 8. MSIS Method. This follows a similar pattern to the USU model showing many of the same structures. However in the MSIS model the highest percent variation in the density is located from mid May, to early June around 75 km. A noted feature in the graph is a region of particularly low density variation located around the summer months from 50 km down to 45 km.

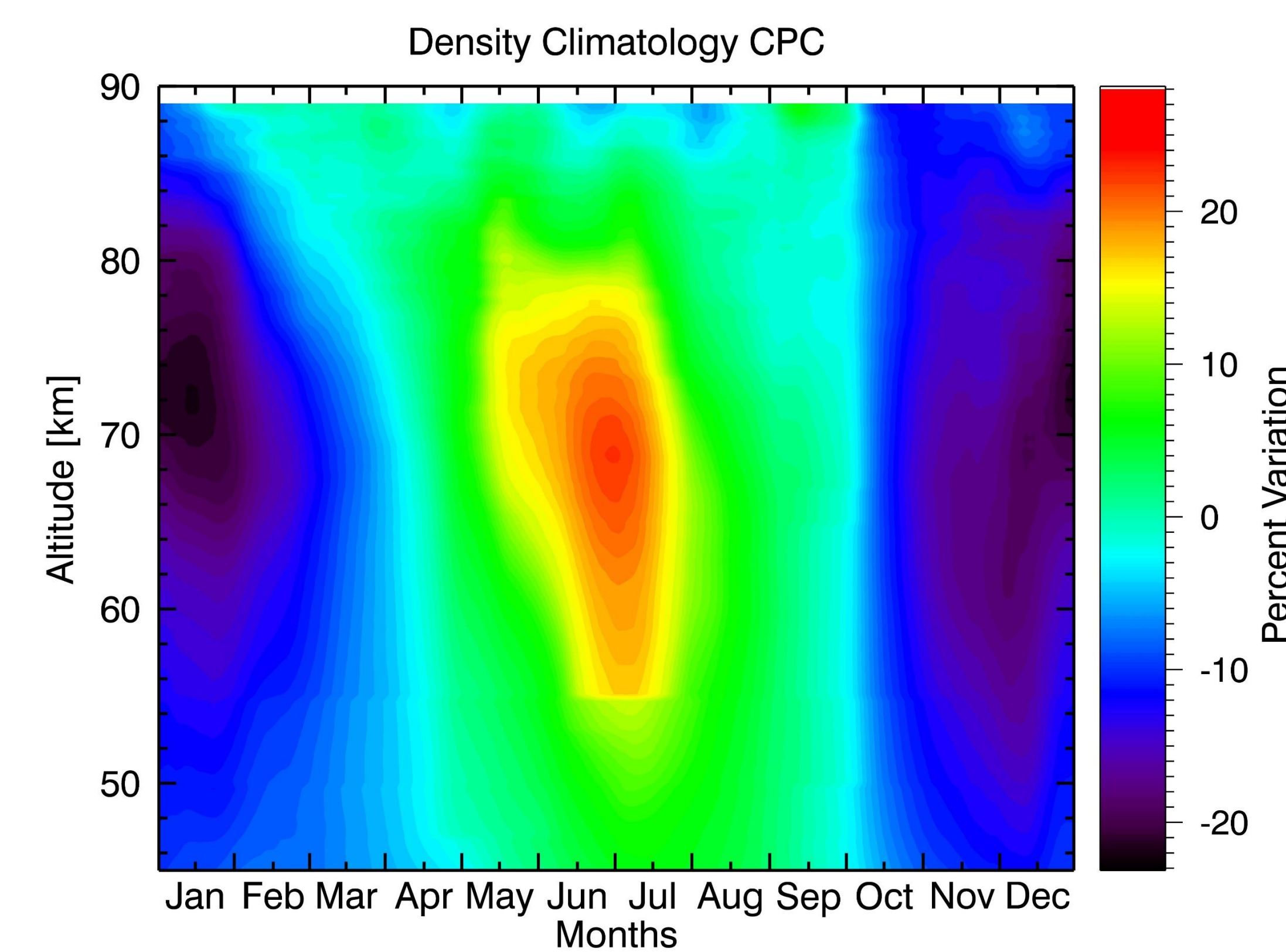


Figure 9. CPC Method. The CPC analysis shows the greatest percent variation. The structure is slightly different than the others in that the low density region over the months June-September is not as obvious, traces of this trend however can still be seen. The peak density is located over June, as shown in the USU model. There also is more seasonal variability at lower altitudes between 45 km and 55 km.

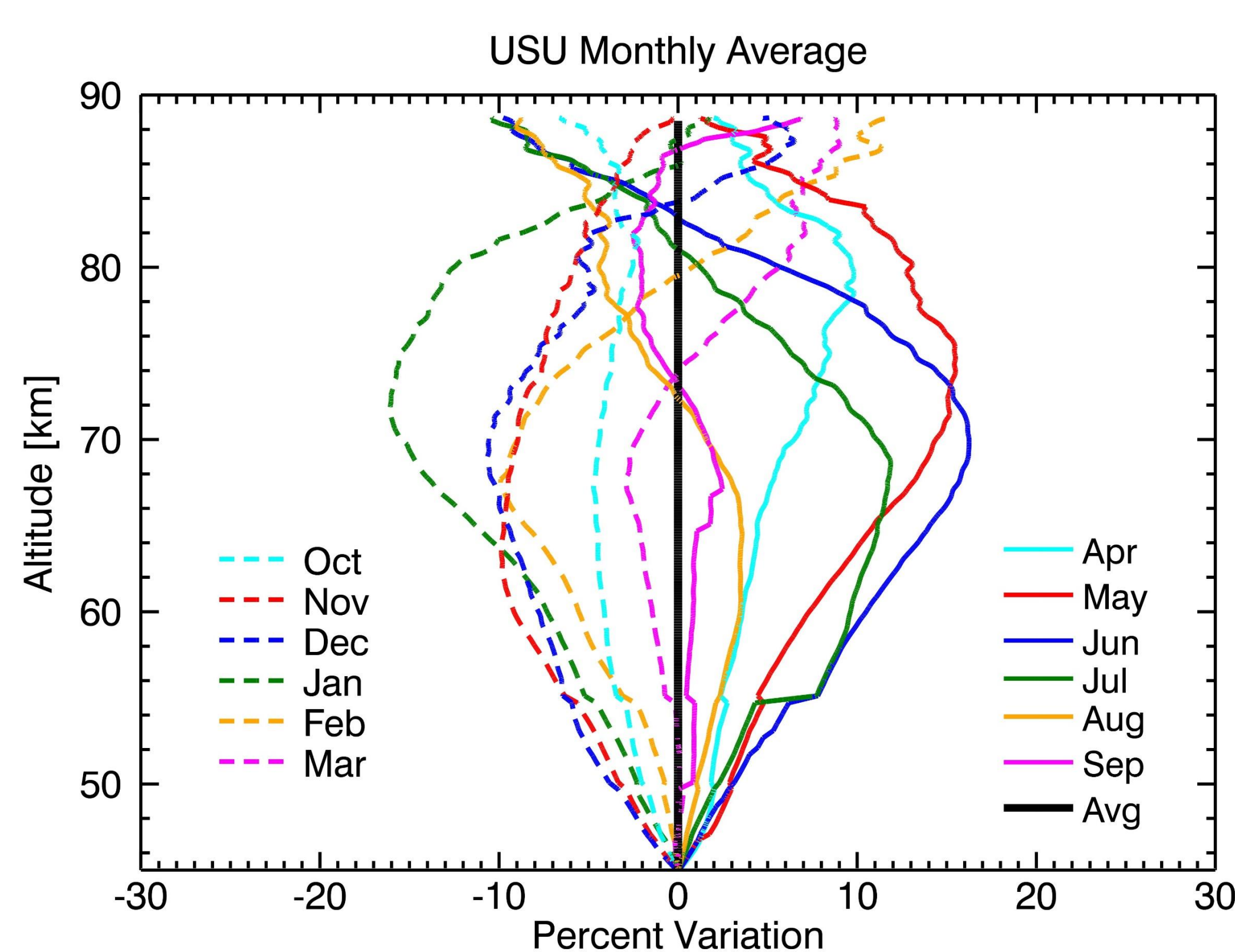


Figure 10. USU Method. The seasonal variation is visible in each month. The large percent difference shown in the month of January versus July, the different between them is roughly 30 percent. This is also similar for the months June and December. Also note that many of the months converge at roughly 85 km

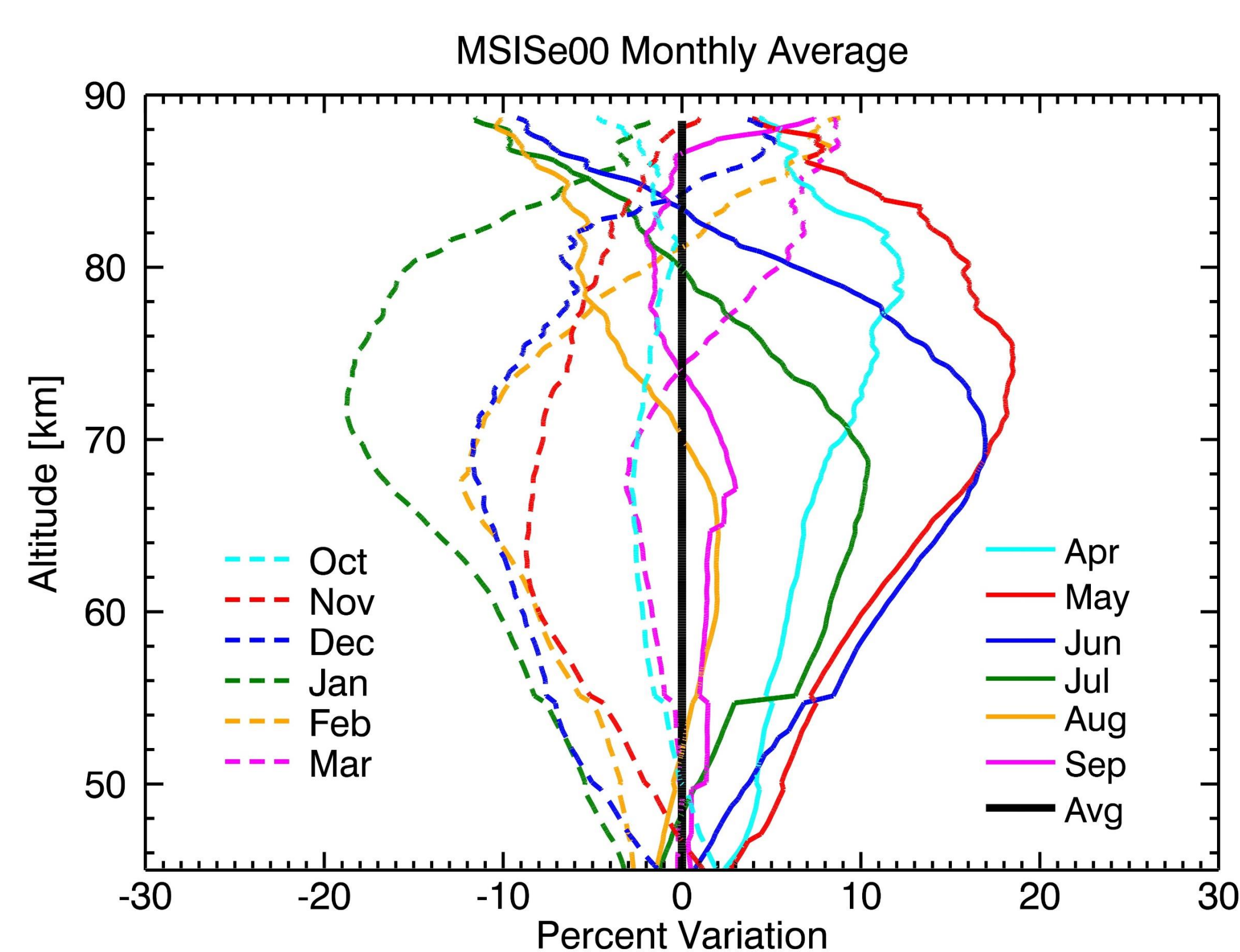


Figure 11. MSIS Method. The seasonal differences are amplified in the MSIS model. The basic shape remains with divergence from the average near the low and mid altitudes, and convergence at the upper altitudes of 85 km. Note that in the MSIS model October and September are very similar up to 70 km, whereas in the USU model they are easily separated.

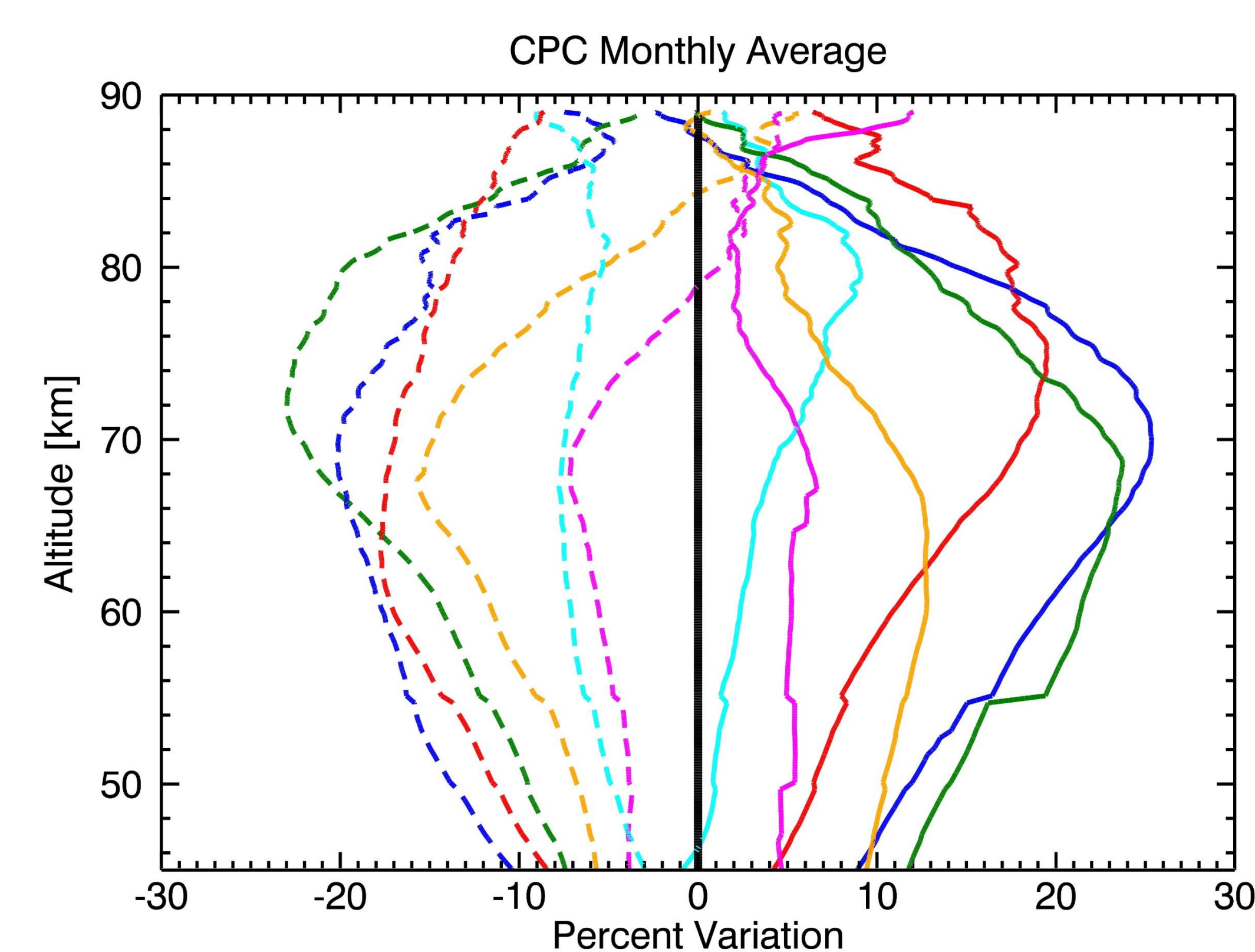


Figure 12. CPC Method. The Monthly averages are amplified most in the CPC analysis. There is almost no convergence of seasonally opposite months with the exception of March and September near 80 km, and February and August at 85 km. The density average also varies great at the lower altitudes by nearly 20 percent between June and January.

Conclusions

Three significantly different normalizations at 45 km were applied to 11 years of relative number density profiles acquired by the Rayleigh lidar at ALO. Despite the different normalizations, many of the same features were seen in the resultant density climatologies.

- What stands out the most are the very high relative densities that peak at approximately the summer solstice and 72 km.
- Very low densities occur near winter solstice at all altitudes and for all of the normalization methods.
- The structure located late summer into early fall that shows a negative density region, extending from 90 km down to 72 km, is not present in all of the analysis methods.
- At the highest altitudes, just below 90 km, the densities are relatively constant throughout the year. However, for a given seasonal period, a bit of a reversal occurs. Relative density minima during a given period, at high altitudes, switch to a maxima at lower altitudes and vice versa.
- The rate of density increase to the summer peak and the fall off afterward are not symmetric. The fall off is slower, showing a secondary peak near fall equinox in both the MSIS and USU normalized results. That is not unexpected in the MSIS normalization because of its semiannual variation at 45 km. Its appearance in the USU normalized densities strengthens the argument that a strong semiannual variation exists in the mesospheric densities. Even in the CPC normalized densities, which are dominated by an annual variation at 45 km, a shoulder is apparent at fall equinox.
- While the absolute maximum in relative densities is near 72 km at summer solstice, the local maxima, in earlier months, occurs at higher altitudes. This earlier appearance at high altitudes is similar behavior to what is seen in the temperatures.
- Another feature that stands out is a very sharp gradient from relatively high relative densities in summer to relatively low densities in winter that occurs almost simultaneously at all altitudes.

Future Work

In addition to the MSISe00 model and CPC analyses, several other models have been developed that will predict the neutral densities at 45 km. The effects of these different normalizations will be explored. These density climatologies can also be used in the study of the ALO temperature data set and the temperature climatology in relation to Sudden Stratospheric Warmings (Sox et al., IAGA 2013 2.5-14). Furthermore, a major upgrade is underway (Wickwar et al., IAGA 2013 2.5-20). It will enable the observations to be carried out to 120 km. This will be exploring to top of what we showed and go significantly into the lower thermosphere. As part of the upgrade, the observations will be extended downward to 15 km. This will provide a much more extensive region of overlap with the meteorological based models to use for normalization.

Acknowledgements

We gratefully acknowledge support from Space Dynamics Lab Internal Research and Development grant program, the Utah NASA Space Grant Consortium Fellowship program, the Howard L. Blood Graduate Scholarship program, Utah State University, the USU College of Science and Physics Department, Personal Contributions and an essential group of volunteers: Marcus Bingham David Barton, Thomas Amely, the Laser Pointers Mechanical Engineering team (Dayne Howard, Ben Maxfield, Rob Neibaur, Ryan Martineau, Mike Hart), Daniel Dunn, Joe Slansky, and Jarod Benowitz.

References

- Picone, J. M., A. E. Hedin, D. P. Drob, and A. C. Aikin, NRLMSISE-00 empirical model of the atmosphere: Statistical comparisons and scientific issues, *J. Geophys. Res.*, 107(A12), 1468, doi:10.1029/2002JA009430, 2002.
- Gelman, M. E., A. J. Miller, K. W. Johnson, and R. N. Nagatani, 1986: Detection of long term trends in global stratospheric temperature from NMC analyses derived from NOAA satellite data. *Adv. Space Res.*, 6, 17-26.
- Herron, J.P. (2007), Rayleigh-Scatter Lidar Observations at USU's Atmospheric Lidar Observatory (Logan, UT) — Temperature Climatology Comparisons with MSIS, and Noctilucent Clouds, PhD Dissertation, Utah State University, Logan, UT.